

A NEW WAY TO LOOK AT FAULT RUPTURE:
UNDERSTANDING AND CHARACTERIZING EARTHQUAKE PREDOMINANT
PERIOD

by
Erik L. Olson

A thesis submitted in partial fulfillment of the requirements for the degree of

Master of Science
(Geology and Geophysics)

at the
UNIVERSITY OF WISCONSIN-MADISON

2005

**A NEW WAY TO LOOK AT FAULT RUPTURE:
UNDERSTANDING AND CHARACTERIZING EARTHQUAKE
PREDOMINANT PERIOD**

Approved by:

Date: _____

Richard M. Allen
Assistant Professor of Geophysics

Table of Contents

Acknowledgements.....	ii
Introduction.....	1
Chapter 1: The Deterministic Nature of Earthquake Rupture.....	3
Introduction	4
Background.....	4
Methods and data	6
Discussion and new hypotheses.....	8
References cited.....	10
Acknowledgements.....	13
Figures.....	13
Table of events studied.....	16
Chapter 2: Characterizing Factors Affecting the Measure of Earthquake Predominant Period.....	19
Abstract.....	20
Introduction.....	20
Study Region.....	21
Data.....	22
Analysis.....	23
Discussion.....	26
References cited.....	27
Acknowledgements.....	28
Figures.....	29
Tables of station corrections.....	39
Conclusions and future work.....	40
Appendix	44

Acknowledgements

This document was made possible by the gracious help of many people. I would like to thank my advisor, Richard Allen for presenting me with the opportunity to pursue cutting edge research that can influence our every day lives. I also thank Richard for his patience, and hands on approach to helping me develop several theories presented here. Cliff Thurber also helped my research significantly, especially in the design and interpretation of the models presented in chapter two.

I would also like to thank my friends and family, both around Madison, and every place I've visited during my time at the University of Wisconsin. Without their support both toward accomplishing my research, and taking a break from it, I would not have been able to complete this document. Thank you to everyone who has helped make this a great experience. I would also like to thank you, for showing interest in my work and reading this text.

INTRODUCTION

Earthquakes are a fascinating phenomenon that over the course of millions of years have changed the face of our planet. Earthquakes remain an enigma, defying scientists' best attempts to characterize their behavior. Until the mid-1900's we could not even fully characterize the size of an earthquake; only through assessing the destruction wrought by the event could we guess at the size of the force. In the late 1930's the magnitude scale arose as a new method of understanding the strength of an earthquake [*Stein and Wysession, 2003*]. Even after the magnitude scale was developed, another 30 years passed before magnitude was tied to earthquake moment, and therefore related to slip on the fault [*Stein and Wysession, 2003*].

Throughout history, even before the size of an earthquake was well understood, people attempted to predict these events. However, calculating the magnitude of an earthquake was not possible, even during the earthquake, let alone prior to rupture initiation. As rupture theory developed, and more earthquakes were studied, scientists began to postulate that the very nature of rupture prevented any fore-warning of an earthquake, and that an earthquake's magnitude could only be determined post-rupture.

Several other theories were proposed contradicting the non-deterministic model of earthquake rupture, however they often failed to explain earthquakes in more than one region, or fell into disfavor after additional research weakened supporting arguments. Then, a few years ago, new empirical evidence appeared which hinted at the possibility of a deterministic rupture process, i.e. evidence that the size of an earthquake may be determined prior to rupture termination. Working with a dataset from California, Allen and Kanamori [2003] found that the predominant period of an earthquake scales with the magnitude of the

earthquake. The maximum predominant period of an earthquake, a value calculated from the frequency content of the P-wave, could be measured in 5 seconds, which is faster than a large earthquake takes to rupture. However, the study of Allen and Kanamori [2003] was limited to a small region, and only included 3 events greater than magnitude 6.

Lockman and Allen [In Review] took the analysis of maximum predominant period a step further and added earthquakes from Japan and the Pacific Northwest to the data set. These additional events remained consistent with the original observations that the maximum predominant period of an earthquake is related to the magnitude of the earthquake. Unfortunately the additional data set did not substantially increase the number of large magnitude events, and the source of predominant period remained an enigma.

The study presented in the following chapters was initiated to pick up the next step in the development of our understanding of predominant period. Despite several years of study, and the publication of many papers on the subject, no one has yet pinned down what causes the earthquake predominant period; nor what process occurs during earthquake rupture initiation that affects the event's final magnitude. This study represents the beginning of this characterization.

References Cited

- Allen, R.M., and H. Kanamori, The potential for earthquake early warning in southern California, *Science*, 300 (5620), 786-789, 2003.
- Lockman, A., and R.M. Allen, Magnitude Period Scaling Relationships for Japan and the Pacific Northwest: Implications for Earthquake Early Warning, *Bulletin of the Seismological Society of America*, In Review.
- Stein, S., and M. Wyssession, *An Introduction to seismology, earthquakes, and earth structure*, 498 pp., Blackwell, Malden, MA, 2003.

CHAPTER 1

The Deterministic Nature of Earthquake Rupture

Erik L. Olson

Department of Geology and Geophysics, University of Wisconsin Madison, 1215 W. Dayton
St., Madison, WI 53706, USA

Submitted to the journal *Nature*

Introduction

Understanding the earthquake rupture process is key to our understanding of fault systems and earthquake hazards. Over the past 15 years multiple hypotheses concerning the nature of fault rupture have been proposed but no unifying theory has emerged¹⁻¹¹. The conceptual hypothesis most commonly cited is the cascade model for fault rupture^{2,6,7,12}. In the cascade model, slip initiates on a small fault patch and continues to rupture further across a fault plane as long as the conditions are favorable. Two fundamental implications of this domino-like theory are that small earthquakes begin in the same manner as large earthquakes, and that the rupture process is not deterministic, i.e., the size of the earthquake cannot be determined until the cessation of rupture. Here we show that the frequency content of radiated seismic energy within the first few seconds of rupture scales with the final magnitude of the event. Therefore the magnitude of an earthquake can be estimated before the rupture is complete. This finding implies that the rupture process is to some degree deterministic and has far-reaching implications for the physics of the rupture process.

Rupture dynamics background

In the cascade model faults are divided into patches of varying size and shape. When an earthquake initiates on one patch, slip on this patch can lead to continued slip on the adjacent patches if the rupture energy and the state of stress on adjacent patches are favorable. An earthquake continues spreading from patch to patch until there is insufficient energy to rupture the next patch at which point the rupture stops. Moment is physically related to both rupture area, A , and average slip, \bar{D} , by the relation $M_o = \mu A \bar{D}$ where M_o is the seismic moment and μ is the shear modulus. Moment magnitude, M_w , scales with the

seismic moment and is therefore similarly related to A and \bar{D} ¹³. Given this framework, it is not possible to know the magnitude of an earthquake until the rupture has stopped.

Throughout the last decade the seismological community has debated whether the first few seconds of the P-wave (the first few seconds of radiated energy) provides information about the final magnitude of an earthquake before the rupture is complete^{3,6,7,10}. Much of the debate has focused on the time-domain characteristics of the P-wave. However, evidence for a scaling relation between the frequency content of the first few seconds of the P-wave and the final magnitude has also emerged¹⁴⁻¹⁷. Using an approach similar to Nakamura¹⁶, Allen and Kanamori¹⁴ measured the predominant period, τ_p , from the first 4 seconds of the P-wave arrival at multiple seismic stations in southern California. τ_p is calculated from the velocity waveform using the following recursive relation

$$\tau_i^p = 2\pi\sqrt{X_i/D_i} \quad (1)$$

where

$$X_i = \alpha X_{i-1} + x_i^2, \quad D_i = \alpha D_{i-1} + \left(\frac{dx}{dt}\right)_i^2, \quad (2)$$

x_i is the ground motion recorded at time i and α is a 1 sec smoothing constant¹⁴. Allen and Kanamori¹⁴ demonstrated a scaling relation between τ_p and magnitude M for earthquakes with M of 3.0 to 7.3. In earthquakes with $M < 6$ the total duration of rupture is usually less than 4 sec, therefore, the entire rupture time history is included within the first 4 sec of the P-wave. However, for $M > 6$ earthquakes, the existence of a scaling relation between τ_p and M would imply that the magnitude of an earthquake has been defined before the rupture terminates and that the rupture process is deterministic. Allen and Kanamori¹⁴ used

earthquakes from southern California where data for only 3 earthquakes with $M_w > 6$ are available.

Methods and data

Here, we measure τ_p for a much larger number of earthquakes including events from Japan, Taiwan, California and Alaska. The waveform data has been provided by K-net operated by the National Research Institute for Earth Science and Disaster Prevention in Japan, the Taiwan Strong Motion Instrumentation Program of the Central Weather Bureau, Southern California Seismic Network operated by Caltech and the US Geological Survey, and the University of Alaska Geophysical Institute. A total of 71 earthquakes producing 1842 waveforms recorded on both broadband velocity sensors and accelerometers within 100 km of the epicenter are used. There are 24 events with $M_w \geq 6.0$, including the M_w 7.6 Chi-Chi earthquake (Taiwan, 1999) with a rupture duration of ~ 30 sec, the M_w 7.9 Denali earthquake (Alaska, 2002) with a rupture duration of ~ 70 sec, and the M_w 8.3 Tokachi-oki earthquake (Japan, 2003) with a rupture duration of ~ 40 sec.

We calculate τ_p in a recursive fashion from a vertical velocity timeseries to generate τ_p as a function of time, $\tau_p(t)$. Figure 1 shows the vertical velocity waveform recorded during a M 4.6 earthquake in southern California and the τ_p timeseries derived from it. Figure 2 shows a similar example but for the M_w 8.3 Tokachi-oki earthquake. In this case only acceleration records are available which have been recursively integrated in a causal fashion to derive the velocity trace from which $\tau_p(t)$ is derived. We define the parameter τ_p^{\max} as the maximum $\tau_p(t)$ data point between 0.05 and 4.0 sec after the P-wave trigger as shown in

Figures 1 and 2. The time window starts at 0.05 rather than 0.00 sec due to the recursive nature of the $\tau_p(t)$ calculation. Using the maximum value between 0.00 and 4.0 can result in leakage of the frequency content of background noise before the P-wave arrival into the time window after the P-wave.

When τ_p^{\max} is plotted against M on a log-linear scale, a scaling relation emerges as shown in Figure 3a. The τ_p^{\max} observations from single waveforms have been averaged for each earthquake using all available data. The best-fit linear relation is

$$\log \tau_p^{\max} = 0.14M - 0.83 \quad (3)$$

and the average absolute deviation of the event averages is 0.54 magnitude units. While there is scatter in the individual event observations, the scaling relation is clear, implying that information about the final magnitude of an earthquake is available within 4 sec of rupture initiation irrespective of the total rupture duration.

A second parameter, τ_d , is also measured from the τ_p timeseries. τ_d is the delay of the τ_p^{\max} observation with respect to the P-wave trigger and is therefore in the range of 0.05 to 4 sec (see Figures 1 and 2). Figure 3b plots the event-averaged τ_d observations versus magnitude which shows a general increase in τ_d with magnitude. Also indicated on Figure 3b is the typical rupture duration of earthquakes as a function of magnitude. This relation shown is only approximate, and is based on scaling relations between rupture length and magnitude. The rupture length is converted to rupture duration by assuming unilateral rupture and a rupture velocity between 2.4 and 3.0 km/s from the estimates of Somerville et al¹⁸. Rupture length may be empirically calculated from earthquake magnitude¹⁹, or estimated from the scaling relationship between moment and stress drop. Both methods are

used here to create the range shown in Figure 3b. The actual rupture duration for a given magnitude event can vary by a factor of 2 or 3. Despite the uncertainty in the rupture duration of the earthquakes included in this study, it is clear that for earthquakes with $M > 4.5$ the τ_p^{\max} observation is made before the rupture has ceased. While up to 4 sec of data are used to determine τ_p^{\max} , the average time window of the P-wave required to determine τ_p^{\max} is less than 2 sec for almost all earthquakes in our study.

Using published moment rate functions for the $M > 6.0$ events in our study we can estimate the amount of moment release at time τ_d . Rupture directivity effects of finite faults mean that the first 2 sec of the P-wave at a given station does not sample exactly 2 sec of the rupture. However, because our τ_d measurement is event-averaged we can use it as an approximate estimate of the rupture duration within which τ_p^{\max} information is available. The amount of seismic moment released within τ_d increases with magnitude, which is not surprising given that τ_d also increases with magnitude. But the percentage of moment released is always small (less than 40% for $M > 6$ events) and decreases with magnitude. In the case of the largest earthquakes, Chi-Chi, Tokachi-oki, and Denali, the percentage of moment released at τ_d is less than 2%.

Discussion and new hypotheses

All of these observations challenge the cascade model for fault rupture. They imply that the beginnings of small and large earthquakes are different, and that the rupture process is at least partly deterministic, i.e. the final magnitude of an event is to some degree controlled by processes within the first few seconds of rupture. While there is scatter in the

τ_p^{\max} data, most events fall within ± 1 magnitude unit of the best-fit line. The scatter could be due to source processes and/or local site and measurement errors. If the scatter is non-source related, then removal or correction for site and path effects could reduce the scatter in the data points of Figure 3a to a single line, implying that the final magnitude of an earthquake is entirely determined within the first 4 sec of rupture. Variability in the quality of the τ_p^{\max} observations at different stations has already been observed across the seismic network in southern California, indicating that site effects do play a role²⁰. Nevertheless, it seems unlikely that all the scatter is due only to site effects. Instead, source related processes including rupture behavior, stress heterogeneity and other on-fault variability probably also play a role.

The τ_p^{\max} observations suggest that the final magnitude of an earthquake is partially controlled by the initiation process within the first few seconds of rupture, and partially by the physical state of the surrounding fault plane. The role played by the initiation process can be understood by considering the energy balance of fault rupture. A rupture can only propagate when the available energy is sufficient to supply the necessary fracture energy^{21,22}. When a propagating fracture encounters a small stress-drop patch, the total energy in the system will begin to decrease. Depending on the size of the patch, rupture may terminate. The total rupture energy available increases with the amount of slip, so a large-slip rupture will propagate further across a heterogeneous fault plane. Therefore, if the rupture pulse initiates with large slip, it is more likely to evolve into a large earthquake. This explanation is also consistent with a recent study of the location of earthquake hypocenter with respect to

the slip distribution. Mai et al.²³ show that hypocenters are preferentially located within or close to regions of large slip.

The τ_p^{\max} scaling relation provides new constraints on the physics of the rupture process. Whereas the cascade model suggests that the magnitude of an earthquake is dependent on the state of stress across the fault plane and that the nucleation of all earthquakes is identical, our new observations demonstrate the significance of the rupture initiation process within the first few seconds of an event. Understanding the physics of this process will enable us to predict the magnitude of earthquakes without the need for accurate knowledge of the surrounding state of stress across a fault plane.

References Cited

1. Beroza, G. C. & Ellsworth, W. L. Properties of the seismic nucleation phase. *Tectonophysics* **261**, 209-227 (1996).
2. Brune, J. N. Implications of earthquake triggering and rupture propagation for earthquake prediction based on premonitory phenomena. *Journal of Geophysical Research* **84**, 2195-2198 (1979).
3. Ohnaka, M. A physical scaling relation between the size of an earthquake and its nucleation zone size. *Pure and Applied Geophysics* **157**, 2259-2282 (2000).
4. Sato, T. & Kanamori, H. Beginning of earthquakes modeled with the Griffith's fracture criterion. *Bulletin of the Seismological Society of America* **89**, 80-93 (1999).
5. Fukao, Y. & Furumoto, M. Hierarchy in earthquake size distribution. *Physics of the Earth and Planetary Interiors* **37**, 149-168 (1985).

6. Ellsworth, W. L. & Beroza, G. C. Seismic evidence for an earthquake nucleation phase. *Science* **268**, 851-855 (1995).
7. Kilb, D. & Gomberg, J. The initial subevent of the 1994 Northridge, California, earthquake: Is earthquake size predictable? *Journal of Seismology* **3**, 409-420 (1999).
8. Mori, J. & Kanamori, H. Initial rupture of earthquakes in the 1995 Ridgecrest, California sequence. *Geophysical Research Letters* **23**, 2437-2440 (1996).
9. Singh, S. K. et al. Implications of a composite source model and seismic-wave attenuation for the observed simplicity of small earthquakes and reported duration of earthquake initiation phase. *Bulletin of the Seismological Society of America* **88**, 1171-1181 (1998).
10. Steacy, S. J. & McCloskey, J. What controls an earthquake's size? Results from a heterogeneous cellular automaton. *Geophysical Journal International* **133**, F11-F14 (1998).
11. Dodge, D. A., Beroza, G. C. & Ellsworth, W. L. Detailed observations of California foreshock sequences: Implications for the earthquake initiation process. *Journal of Geophysical Research-Solid Earth* **101**, 22371-22392 (1996).
12. Ellsworth, W. L. & Beroza, G. C. Observation of the seismic nucleation phase in the Ridgecrest, California, earthquake sequence. *Geophysical Research Letters* **25**, 401-404 (1998).
13. Kanamori, H. The energy release in great earthquakes. *Journal of Geophysical Research* **82**, 2981-2987 (1977).
14. Allen, R. M. & Kanamori, H. The potential for earthquake early warning in southern California. *Science* **300**, 786-789 (2003).

15. Kanamori, H. The diversity of the physics of earthquakes. *Proceedings of the Japan Academy Series B* **80**, 297-316 (2004).
16. Nakamura, Y. On the urgent earthquake detection and alarm system (UrEDAS). *Ninth World Conference on Earthquake Engineering VII*, 673-678 (1988).
17. Nakamura, Y. UrEDAS, Urgent earthquake detection and alarm system, now and future. *13th World Conference on earthquake Engineering Paper No. 908* (2004).
18. Somerville, P., Irikura, K., Graves, R. P., Sawada, S. & Wald, D. Characterizing crustal earthquake slip models for the prediction of strong motion. *Seismological Research Letters* **70**, 59-80 (1999).
19. Wells, D. L. & Coppersmith, K. J. New empirical relationships among magnitude, rupture length, rupture width, rupture area, and surface displacement. *Bulletin Of The Seismological Society Of America* **84**, 974-1002 (1994)
20. Lockman, A. & Allen, R. M. Single station earthquake characterization for early warning. *Bulletin of the Seismological Society of America* (in review).
21. Nielsen, S. B. & Olsen, K. B. Constraints on stress and friction from dynamic rupture models of the 1994 Northridge, California, earthquake. *Pure and Applied Geophysics* **157**, 2029-2046 (2000).
22. Oglesby, D. D. & Day, S. M. Stochastic fault stress: Implications for fault dynamics and ground motion. *Bulletin of the Seismological Society of America* **92**, 3006-3021 (2002).
23. Mai, P. M., Spudich, P. & Boatwright, J. Hypocenter locations in finite-source rupture models. *Bulletin of the Seismological Society of America* (in press).

Acknowledgements

I thank Hiroo Kanamori and Stefan Nielsen for helpful discussions, and Yih-Min Wu and Roger Hansen for making waveform data available for the study. Funding for this work was provided by USGS/NEHRP awards 03HQGR0043 and 05HQGR0074, and by the University of Wisconsin – Madison.

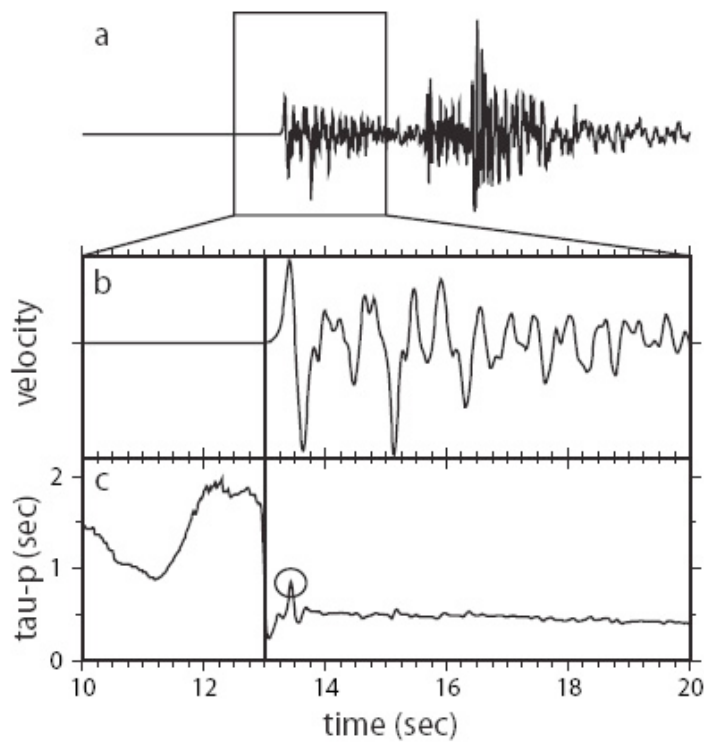


Figure 1. Example waveform and τ_p^{\max} calculation for a M 4.6 earthquake in southern California recorded at station GSC 74 km from the epicenter. **a**, The raw vertical component waveform recorded by a broadband velocity sensor. **b**, Ten seconds of the velocity waveform after low-pass filtering at 3 Hz. The P-wave trigger time is shown by the vertical line at 13.01 sec. **c**, $\tau_p(t)$ trace calculated in a recursive fashion from the waveform in **b** showing the

change in the frequency content from the pre-trigger noise to the post-trigger P-wave. The τ_p^{\max} observation is circled (equal to 0.86 sec in this case), τ_d is the delay of τ_p^{\max} with respect to the trigger (0.43 sec in this case).

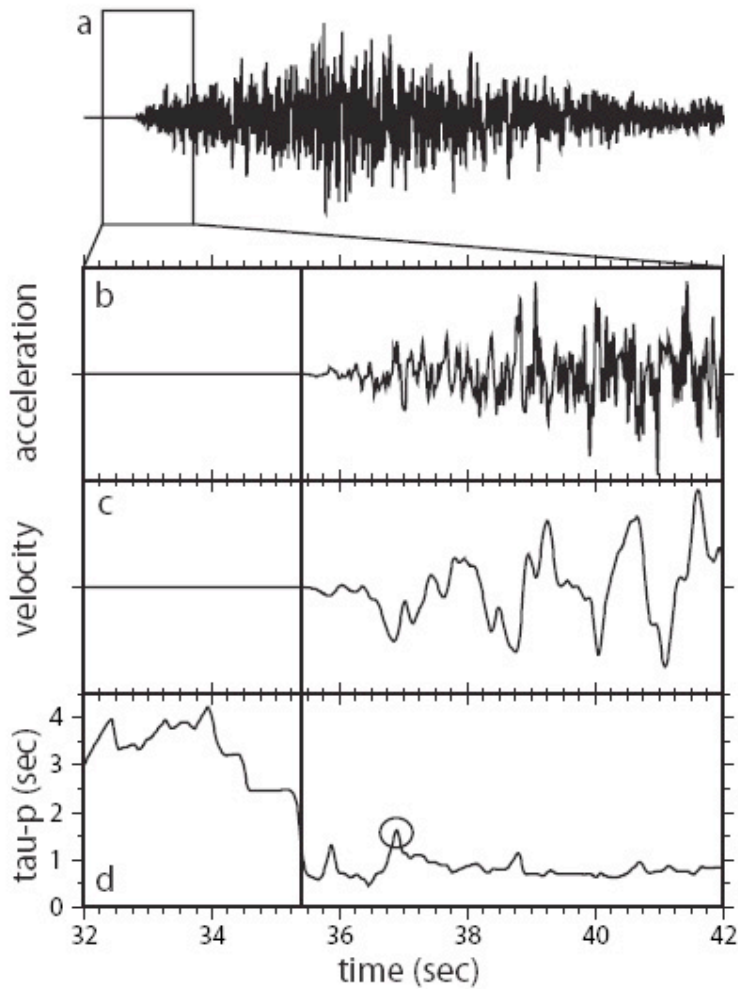


Figure 2. Example waveform and τ_p^{\max} calculation for the M_w 8.3 Tokachi-oki earthquake recorded at station HKD112 71 km from the epicenter. **a**, The raw vertical component waveform recorded on an accelerometer. **b**, Ten seconds of the raw acceleration waveform.

The P-wave trigger is shown by the vertical line at 35.41 sec. **c**, Ten seconds of the velocity waveform determined from the acceleration recording using recursive relations only. It has also been low-pass filtered at 3 Hz. **d**, $\tau_p(t)$ trace calculated in a recursive fashion from the waveform in **c**. The τ_p^{\max} observation is circled ($\tau_p^{\max} = 1.62$ sec, $\tau_d = 1.49$ sec), it has a longer period and is observed later than the example in Figure 1c due to the larger magnitude of the earthquake.

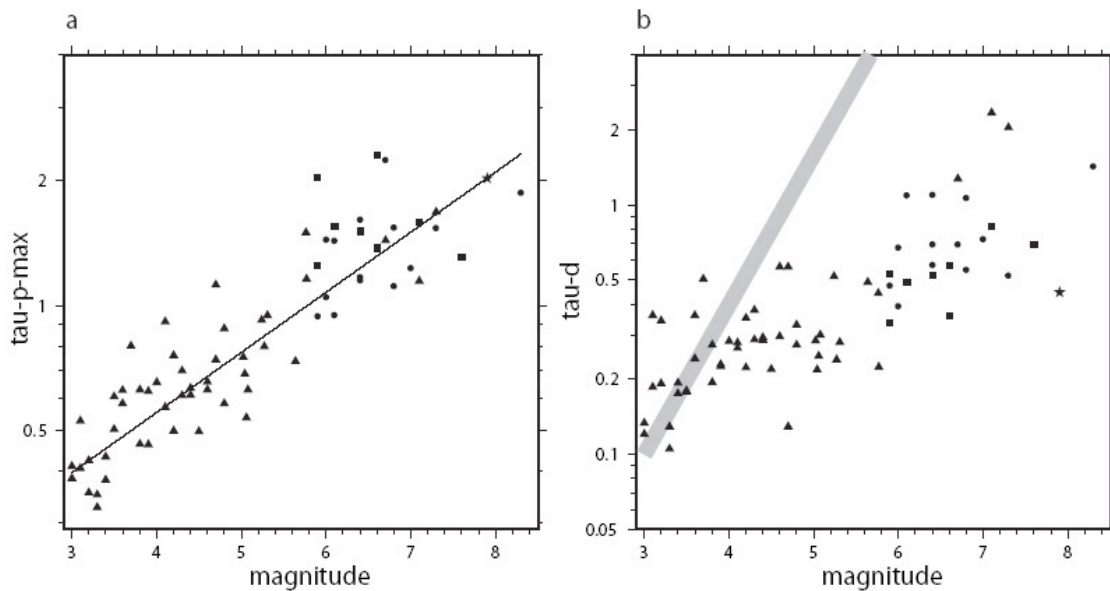


Figure 3. The relation between τ_p^{\max} , τ_d and magnitude. **a**, The scaling relation between event averaged τ_p^{\max} and magnitude for earthquakes in southern California (triangles), Japan (circles), Taiwan (squares) and Alaska (star). The best fit line is also shown; the average absolute deviation of the observations is 0.54 magnitude units. **b**, τ_d plotted against magnitude showing the general increase in the time required to make the τ_p^{\max} observation with increasing magnitude. The symbols are the same as in **a**. The grey bar shows the

approximate rupture duration as a function of magnitude indicating that the τ_p^{\max} observation is made before rupture ceases for all $M > 4.5$ earthquakes.

Table 1

Earthquakes included in this study

Region	Date	Time (UTC)	Magnitude	Latitude	Longitude	tau- p- max	tau- d
Alaska (Denali)	11/03/02	22:11:57.88	7.9	63.52	-147.53	2.02	0.45
Taiwan (Chi- Chi)	09/20/99	17:47:15.85	7.6	23.85	120.82	1.31	0.69
Taiwan	09/20/99	18:03:41.57	6.6	23.80	120.86	2.29	0.58
Taiwan	09/20/99	18:16:17.95	6.6	23.86	121.04	1.37	0.36
Taiwan	06/10/00	18:23:29.45	6.4	23.90	121.11	1.51	0.52
Taiwan	06/14/01	02:35:35.78	5.9	24.42	121.93	2.03	0.53
Taiwan	03/31/02	06:52:49.95	7.1	24.14	122.19	1.59	0.82
Taiwan	05/15/02	03:46:05.91	6.1	24.56	121.87	1.55	0.49
Taiwan	06/10/03	08:40:32.05	5.9	23.50	121.70	1.25	0.34
Japan	01/28/00	14:21:07.34	6.8	42.98	146.72	1.54	1.07
Japan	06/03/00	08:54:49.20	6.1	35.68	140.72	1.43	1.10
Japan	06/06/00	21:16:42.40	5.9	36.84	135.55	0.94	0.48
Japan	07/20/00	18:39:18.82	6.0	36.52	141.10	1.44	0.67
Japan	03/24/01	06:27:53.58	6.8	34.12	132.71	1.12	0.55
Japan	08/13/01	20:11:23.40	6.4	41.01	142.42	1.61	0.70
Japan	11/03/02	03:37:42.07	6.4	38.89	142.14	1.17	0.58
Japan	05/26/03	09:24:33.40	7.0	38.80	141.68	1.23	0.73
Japan	07/25/03	22:13:29.97	6.0	38.40	141.17	1.05	0.39
Japan (Tokachi- Oki)	09/25/03	19:50:06.36	8.3	41.78	144.08	1.87	1.43
Japan	09/25/03	21:08:00.03	7.3	41.71	143.69	1.54	0.52
Japan	09/29/03	02:36:53.14	6.4	42.36	144.56	1.15	1.10
Japan	10/08/03	09:06:55.34	6.7	42.56	144.67	2.24	0.70
Japan	12/29/03	01:30:54.70	6.1	42.42	144.76	0.95	0.49
California (Landers)	06/28/92	11:57:34.12	7.3	34.20	-116.44	1.68	2.05
California (Northridge)	01/17/94	12:30:55.00	6.7	34.21	-118.54	1.44	1.27
California	09/20/95	23:27:36.30	5.8	35.76	-117.64	1.50	0.44

California	11/27/96	20:17:24.01	5.3	36.08	-117.65	0.95	0.28
California	03/18/97	15:24:47.07	5.3	34.97	-116.82	0.80	0.24
California	04/26/97	10:37:30.07	5.1	34.37	-118.67	0.63	0.30
California	03/06/98	05:47:40.03	5.2	36.07	-117.64	0.92	0.52
California	03/07/98	00:36:46.08	5.0	36.08	-117.62	0.69	0.22
California (Hector Mine)	10/16/99	09:46:44.01	7.1	34.60	-116.27	1.14	2.35
California	10/16/99	09:59:35.02	5.8	34.68	-116.29	1.16	0.22
California	10/16/99	10:20:52.01	4.8	34.36	-116.15	0.58	0.28
California	10/16/99	11:26:04.01	4.7	34.81	-116.34	0.74	0.13
California	10/16/99	12:57:21.10	5.6	34.44	-116.24	0.74	0.49
California	10/16/99	20:13:37.01	4.6	34.69	-116.28	0.66	0.30
California	10/16/99	22:53:41.00	4.5	34.71	-116.35	0.50	0.22
California	10/21/99	01:54:34.02	5.1	35.27	-116.07	0.54	0.25
California	10/22/99	16:08:48.01	5.0	34.87	-116.41	0.75	0.29
California	02/21/00	13:49:43.00	4.3	34.05	-117.26	0.61	0.29
California	05/11/00	21:46:07.01	3.1	33.84	-117.74	0.53	0.36
California	06/26/00	15:43:07.01	4.6	34.78	-116.29	0.63	0.56
California	09/16/00	13:24:41.00	3.2	33.98	-118.42	0.36	0.19
California	01/14/01	02:26:14.00	4.3	34.28	-118.40	0.70	0.38
California	02/13/01	03:04:35.01	3.5	34.55	-117.43	0.61	0.18
California	02/18/01	06:09:32.00	3.3	33.68	-116.81	0.33	0.11
California	03/25/01	00:41:25.00	3.4	34.05	-117.57	0.38	0.19
California	04/13/01	11:50:12.00	3.6	33.88	-117.69	0.63	0.36
California	04/20/01	09:52:12.00	3.4	33.71	-116.78	0.43	0.18
California	04/30/01	23:34:17.01	3.7	36.05	-117.88	0.80	0.51
California	05/14/01	17:13:30.00	3.8	34.23	-117.44	0.47	0.28
California	05/17/01	22:56:45.01	4.1	35.80	-118.05	0.57	0.27
California	07/03/01	11:40:48.00	3.9	34.26	-116.76	0.46	0.23
California	07/17/01	12:59:59.00	4.7	36.02	-117.88	1.12	0.56
California	07/17/01	12:07:26.00	4.8	36.01	-117.86	0.88	0.33
California	07/20/01	12:53:07.00	4.4	36.00	-117.88	0.61	0.29
California	08/20/01	07:34:23.00	3.0	34.04	-117.25	0.39	0.13
California	09/09/01	23:59:18.00	4.2	34.06	-118.39	0.76	0.35
California	09/17/01	01:14:49.00	3.1	33.92	-117.77	0.41	0.19
California	10/28/01	16:27:45.01	4.0	33.92	-118.27	0.65	0.28
California	10/28/01	16:29:54.01	3.0	33.93	-118.30	0.41	0.12
California	11/13/01	20:43:14.01	4.1	33.32	-115.70	0.92	0.28
California	01/29/02	06:08:01.01	3.8	34.37	-118.66	0.63	0.20
California	01/29/02	05:53:28.01	4.2	34.36	-118.66	0.50	0.22
California	01/29/02	20:23:07.00	3.6	34.36	-118.67	0.58	0.24
California	01/29/02	06:00:39.01	3.9	34.37	-118.67	0.62	0.23
California	01/30/02	18:47:57.00	3.5	34.37	-118.66	0.50	0.18
California	03/17/02	05:50:43.00	3.2	33.87	-117.86	0.43	0.34

California	04/05/02	08:02:56.00	4.4	34.52	-116.30	0.63	0.29
California	07/01/02	22:03:59.01	3.3	34.10	-116.65	0.35	0.13

CHAPTER 2**Fundamental Controls on the Behavior of Earthquake Predominant Period**

Erik L. Olson

Department of Geology and Geophysics, University of Wisconsin Madison, 1215 W. Dayton
St., Madison, WI 53706, USA

Abstract

Earthquake predominant period is a new characteristic of earthquakes that scales with earthquake magnitude. Previous studies describing predominant period (τ_p^{\max}) focused on the relationship between τ_p^{\max} and magnitude, but did not examine factors that potentially control the behavior of τ_p^{\max} . The nature of earthquake rupture, the path of emitted seismic waves, and site effects around a seismometer may all influence the recorded τ_p^{\max} values for an earthquake. These effects may be a source of noise, and scatter, in the τ_p^{\max} trend, limiting our understanding of the relationship between τ_p^{\max} and magnitude. The island of Taiwan represents an ideal location to study effects on τ_p^{\max} due to the dense station coverage, and large number of earthquakes in the region. Through examining the spatial relationships of τ_p^{\max} recorded for several earthquakes around Taiwan, I demonstrate that local site effects, such as geology and structure may influence the average τ_p^{\max} value for an earthquake. These spatial relationships also suggest that the directive nature of rupture influences the average τ_p^{\max} for an event. One way to remove the effects mentioned above is through station correction factors obtained through data inversion. Unfortunately, the data set for Taiwan is currently too sparse for the derivation of reliable station corrections. However, the addition of more earthquakes to the data set will help constrain correction factors needed in Taiwan, and help the analysis of other global data sets.

Introduction

Earthquake predominant period is a versatile new characteristic that can be measured in the first four seconds of earthquake rupture. Research demonstrates that the maximum

predominant period measured in the first four seconds of an earthquake (τ_p^{\max}) scales with the magnitude of an earthquake (figure 1), and that constructing an early warning system that uses τ_p^{\max} can help mitigate some seismic hazard [*Allen and Kanamori, 2003; Lockman and Allen, In Review; Lockman and Allen, In Review; Olson and Allen, In Review*]. However τ_p^{\max} remains an empirical measurement that lacks a fundamental explanation in relation to the rupture that creates the signal. Additionally, while factors affecting the seismic waveform that carries the τ_p^{\max} signal have been studied for several decades, factors that affect τ_p^{\max} remain unknown.

Site effects, ray path geometry and geology, and rupture directivity are just a few of the factors known to effect the seismic signal recorded at a station. All of these factors were studied at locations around the world, and geoscientists derived correction factors to compensate for many effects of these factors. τ_p^{\max} however, is a new characteristic, so the effects of station location, ray path geometry, and rupture directivity are all unknown.

Study Region

The island of Taiwan represents an ideal location to study the fundamental controls on the behavior of τ_p^{\max} . Due to numerous large earthquakes that occur in the region, local geoscientists installed several hundred seismic stations to study the events. These stations are well distributed across the island covering most of the region with the exception of the central mountains (Figure 2). These stations have recorded hundreds of earthquakes, including 8 events greater than magnitude 5.9 since 1999, on or within 50 km of the island.

Eventually a global study of controls on τ_p^{\max} will be required, but Taiwan represents a good area to initiate this study. The Taiwan region has several strengths, mentioned above, but also has a few weaknesses when compared with other seismic regions around the globe. Only a few large magnitude earthquakes occurred in Taiwan over the past several years, and two of the larger events are aftershocks of the Chi Chi earthquake. Additionally, none of these large earthquakes represent a well known directive earthquake, such as Hector Mine (October, 1999, California), and Denali (November 2002, Alaska). A well studied directive rupture would allow a detailed examination of the directivity effect on τ_p^{\max} .

Data

τ_p^{\max} is related to earthquake magnitude (figure 1)[*Allen and Kanamori, 2003; Lockman and Allen, In Review; Lockman and Allen, in review; Olson and Allen, In Review*]. However the relation presented by Olson and Allen [In Review] shows a significant amount of scatter, allowing τ_p^{\max} to only predict the magnitude within a ± 1 magnitude unit scatter (figure 1). They hypothesized the two most probable sources of scatter are site effects and source effects. Source effects are related to the fault rupture, and may be caused by factors such as fault plane asperities, in-fault materials such as gouge or clay, and the nature of patch rupture. Although these effects can be studied in greater detail, no amount of research will allow correction for the scatter they cause, as each earthquake ruptures a fault in a new way.

Site effects, such as station geology, station noise levels, and perhaps even nearby structures such as basins could potentially be corrected for, therefore reducing the scatter of τ_p^{\max} . To analyze these effects, we gathered data from 8 large (greater than magnitude 5.9)

earthquakes in the Taiwan region. These 8 earthquakes were recorded at over 300 stations across the island, and provide a large data set to work with for examining station effects (Figure 2).

Analysis

One qualitative way to examine site effects that control τ_p^{\max} measurements is to plot τ_p^{\max} at each station that recorded one particular earthquake on a regional map (Figures 3-8). Examining these maps provides a first order estimate of numerous possible site effects. A cluster of stations recording anomalously high or low τ_p^{\max} values may be indicative of a regional effect, such as local geology or structure. If the cluster is within a relatively uniform region, geologically, then the cluster of anomalous stations may be indicative of path effects, that only effect a small azimuth range away from the main shock. Two events that occur in the central portion of the island do not produce regular deviations in τ_p^{\max} values (Figures 3 and 4). While one region may record anomalously low τ_p^{\max} values in one earthquake, the next earthquake recorded in the region displays no such trend.

The events mapped in figures 4 and 5 both show patterns for τ_p^{\max} deviation. In both cases, the region of Taiwan centered around 25° latitude and 121.2° longitude contains stations that consistently measure τ_p^{\max} values higher than the mean. This phenomenon may be due to regional structures, or the type of rock in the area. These stations are largely confined to a basin north of the central mountain range. However, stations located in other basins throughout the island do not show similar behavior (e.g. southwestern stations in

figure 4), so a more detailed study of the regional structure effects is required. Studying the τ_p^{\max} deviation maps for other events triggering these northwestern stations would also help find the source of the anomaly in this region. If maps of τ_p^{\max} from events occurring north or west of this anomalous region, do not show a similar trend to figures 5 and 6 then perhaps the anomaly is caused by a structure between the events off the east coast of Taiwan, and the stations in the northwest.

The station anomaly pattern in figure 7 resembles the pattern that would be produced by directive earthquake rupture. Stations south of the event record a higher than average τ_p^{\max} , while stations north of the event record a lower than average τ_p^{\max} . Many of the stations in figure 7 also recorded the events shown in figures 3-6, and for those events these stations do not show a similar pattern. Therefore, only the earthquake mapped in figure 7 is responsible for the observed pattern, rather than regional geology or structure. If this event ruptured along a fault from south to north, the Doppler effect would cause stations south of the earthquake to measure lower than average frequencies (higher periods), and the stations to the north would measure higher than average frequencies (lower periods). The anomaly pattern in figure 7 may be evidence of this Doppler shift. However, due in part to the small size of this earthquake, researchers have not determined whether or not this earthquake ruptured in a unilateral manner. So the apparent directivity signal of figure 7 may just be a random anomaly pattern.

A more quantitative way to evaluate station effects controlling τ_p^{\max} is to invert for station corrections. For example, if one station consistently recorded anomalously high τ_p^{\max}

values, the correction for that station would lower the τ_p^{\max} value, bringing the station closer to the best fit line of Olson and Allen [In Review]. Here we invert for both a station correction and the best fit line between all of the data, using the same data set as Olson and Allen (submitted). All of the data are used to constrain the best fit line, while only data from Taiwan are used to analyze station corrections. The only constraint on a station correction comes from the number of events recorded at that station. For this reason, we only inverted for station corrections at stations that recorded at least 3 events. We also tried more constrained data sets, inverting for corrections at stations with at least 4, 5, and 6 events being recorded. Ideally every station used in the study would record every event, allowing for the maximum constraint on τ_p^{\max} , however we limited our study to only include stations within 100km of the earthquake epicenter. Therefore, very few stations recorded all 8 events, and only when we step back to a requirement of 3 or more events do we achieve a suitable percentage of total stations.

The inversion method used is a SVD pseudo-inverse. The inversion solves for the a and b values of the best fit line given by $y = ax + b$, and the correction factor for each Taiwan station recording at least the minimum number of events. Table 1 shows the number of data, and number of model parameters inverted for with each different minimum number of events. Using the standard deviation of the inversion residuals, we developed a 95% confidence interval for each one of the model parameters. Comparing the 95% confidence interval with the size of the station correction demonstrates that this problem is poorly constrained. The 95% confidence uncertainty range is larger than the correction factor in almost all cases (Table 2). However, the best fit line parameters that were analyzed, a and b,

have very small uncertainty relative to their size, suggesting these two model parameters are well constrained. To achieve constraint on the station corrections similar to those of a and b, a much larger data set is required for the Taiwan region. Increasing from at least 3 events to at least 6 minimum events only slightly improves the constraint, so several more earthquakes are required, perhaps as many as twenty or thirty more to constrain the station correction factors. Figures 9 and 10 are maps of the correction factors calculated from the inversions requiring a minimum of 3 events, and a minimum of 4 events.

Another shortcoming of the inversion is the trade-off allowed between model parameters. The off diagonal elements of the correlation matrix are large, suggesting that many of these corrections trade off. Again, a larger number of events may help constrain the problem, but there will always be a certain amount of trade-off in these values.

Discussion

The maps of τ_p^{\max} deviation from event averages (figures 3-8) highlight many of the station effects that may be influencing τ_p^{\max} . Stations in certain areas of Taiwan appear to consistently measure anomalous τ_p^{\max} values (figures 5 and 6), and one anomaly pattern suggests the possibility of rupture directivity effecting τ_p^{\max} (figure 7). However, a more detailed study, including several more moderate to large earthquakes ($M > 5.0$) is required before any of these patterns can be thoroughly understood. With only two events being recorded at the northwestern Taiwan stations (figures 5 and 6) the evidence for a geologically sourced τ_p^{\max} anomaly is weak. To study the effect of rupture directivity on τ_p^{\max} , the event shown in figure 7 is not the best starting point. Other regions of the world, such as Turkey,

and California, experienced several large earthquakes recently which are known to have ruptured in one direction. These well studied events would be the best starting place for a study in rupture directivity.

Station correction factors derived to identify and correct for any station showing consistent deviation from average τ_p^{\max} values are too poorly constrained to significantly reduce scatter in the τ_p^{\max} - magnitude trend presented by Olson and Allen. Similar to the maps discussed above, expanding the data set by adding more moderate sized earthquakes may help constrain these correction factors.

The preliminary evidence discussed above, both from the station correction factors and maps of τ_p^{\max} suggests that τ_p^{\max} is influenced by station effects. Eventually correcting for these effects through the use of a larger data set will potentially reduce the scatter in τ_p^{\max} period relationship, allowing a more accurate rapid estimation of magnitude. These corrections could eventually lead to a more complete understanding of rupture initiation.

References Cited

- Allen, R.M., and H. Kanamori, The potential for earthquake early warning in southern California, *Science*, 300 (5620), 786-789, 2003.
- Lockman, A., and R.M. Allen, Magnitude Period Scaling Relationships for Japan and the Pacific Northwest: Implications for Earthquake Early Warning, *Bulletin of the Seismological Society of America*, In Review.
- Lockman, A., and R.M. Allen, Single station earthquake characterization for early warning, *Bulletin of the Seismological Society of America*, in review.
- Olson, E.L., and R.M. Allen, The Deterministic Nature of Earthquake Rupture, *Nature*, In Review.

Acknowledgements

I would like to thank Richard Allen, Cliff Thurber, Michael Brudzinski, and Heather DeShon for many helpful discussions that significantly improved this paper. Funding for this work was provided by USGS/NEHRP awards 03HQGR0043 and 05HQGR0074, and by the University of Wisconsin – Madison.

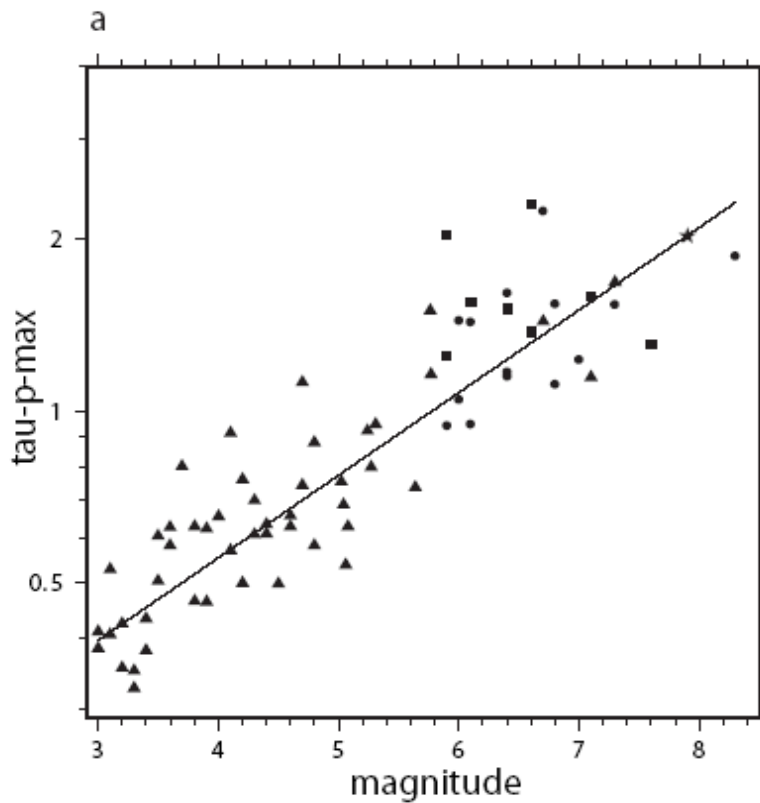


Figure 1. The scaling relationship between event averaged τ_p^{\max} and earthquake moment magnitude (from Olson and Allen [In Review]). Earthquakes from California (triangles), Japan (circles), Taiwan (squares), and Alaska (star) all follow a similar relationship between magnitude and period. The scatter is approximately ± 1 magnitude unit.

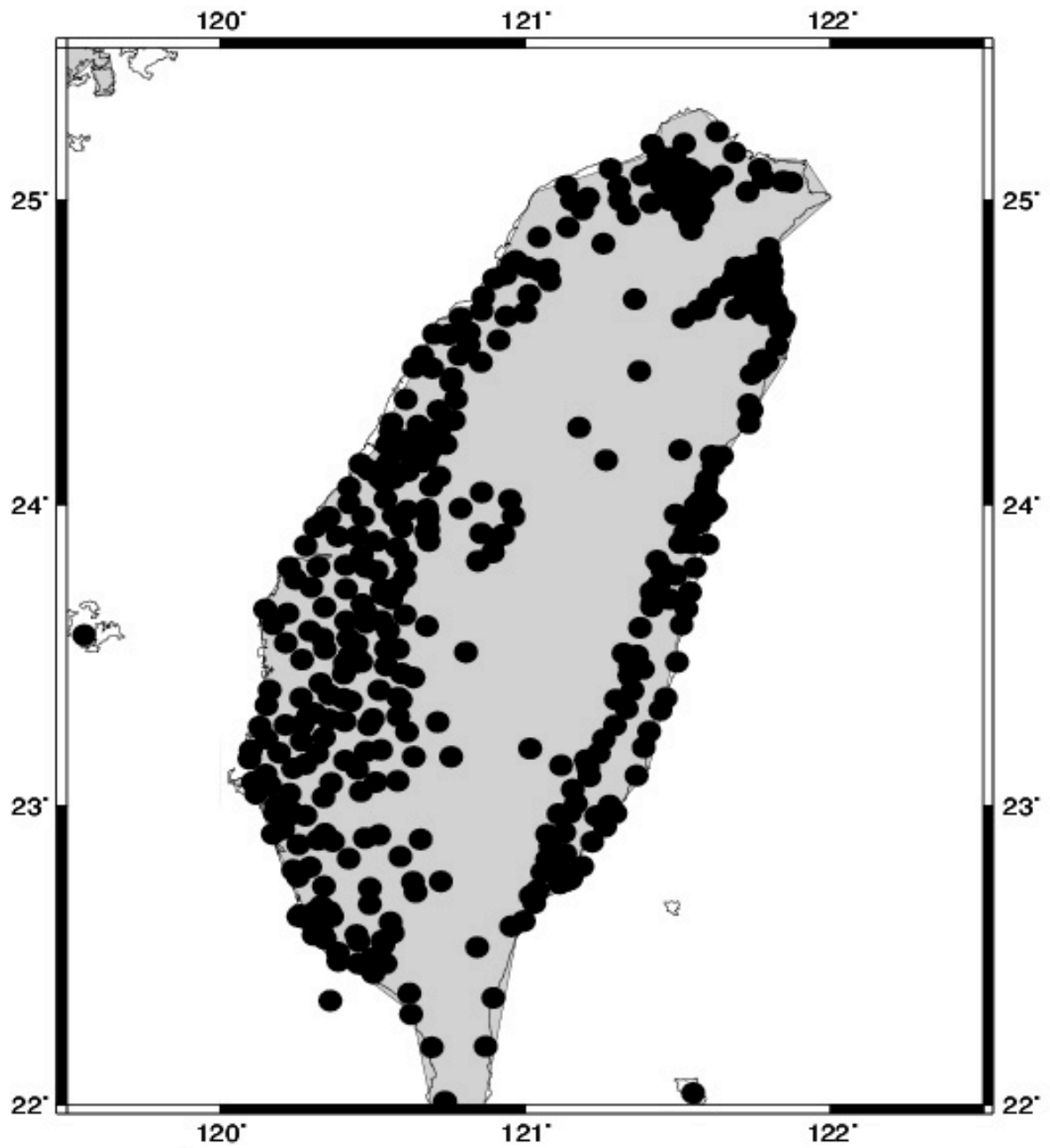


Figure 2. Map of Taiwan, and all of the seismic stations currently installed on the island.

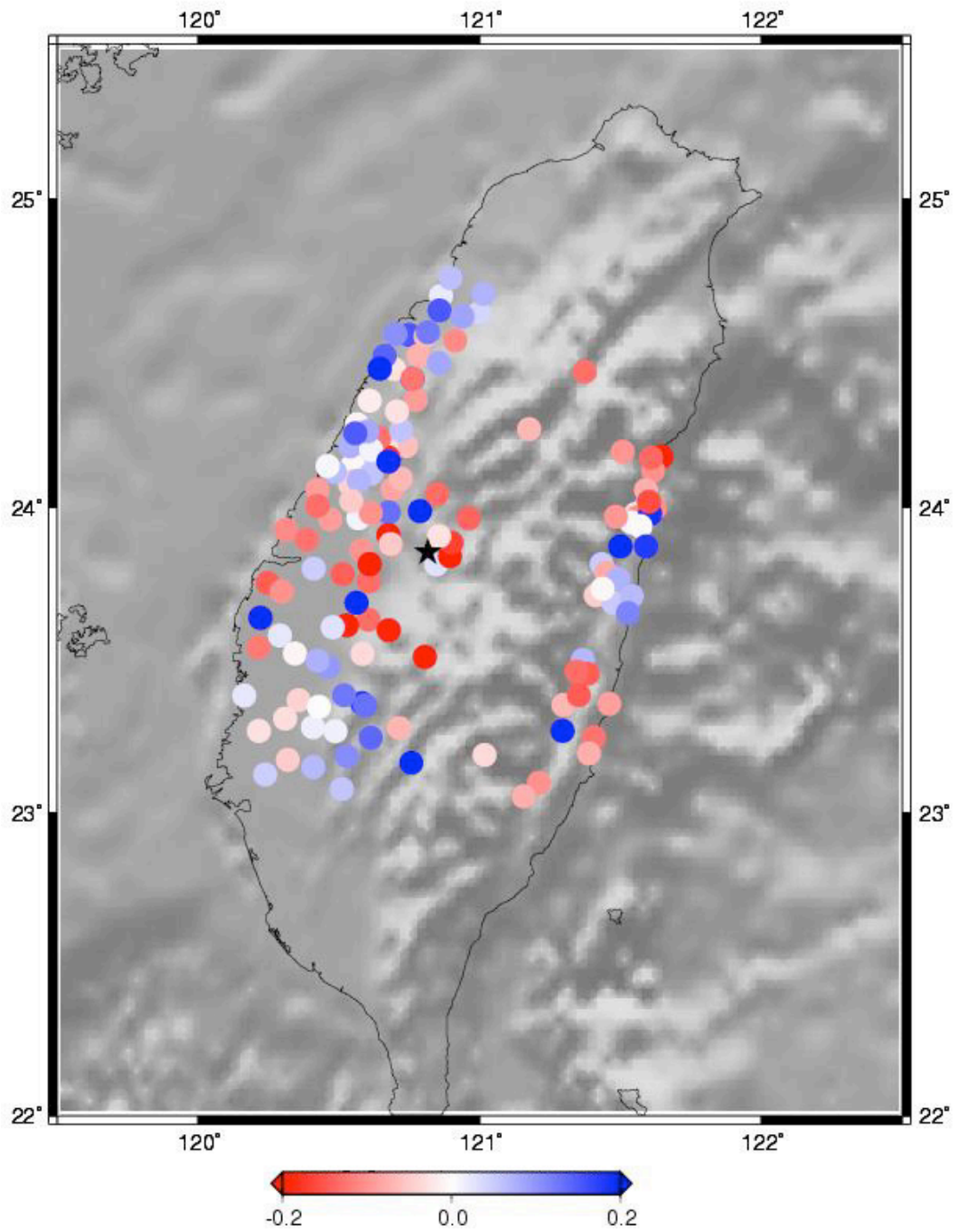


Figure 3. Map of stations within 100km of the M7.6 Chi Chi earthquake that occurred September 20th 1999. The color scale illustrates $\log_{10}(\tau_p^{\max})$ deviation from the mean τ_p^{\max} for this earthquake.

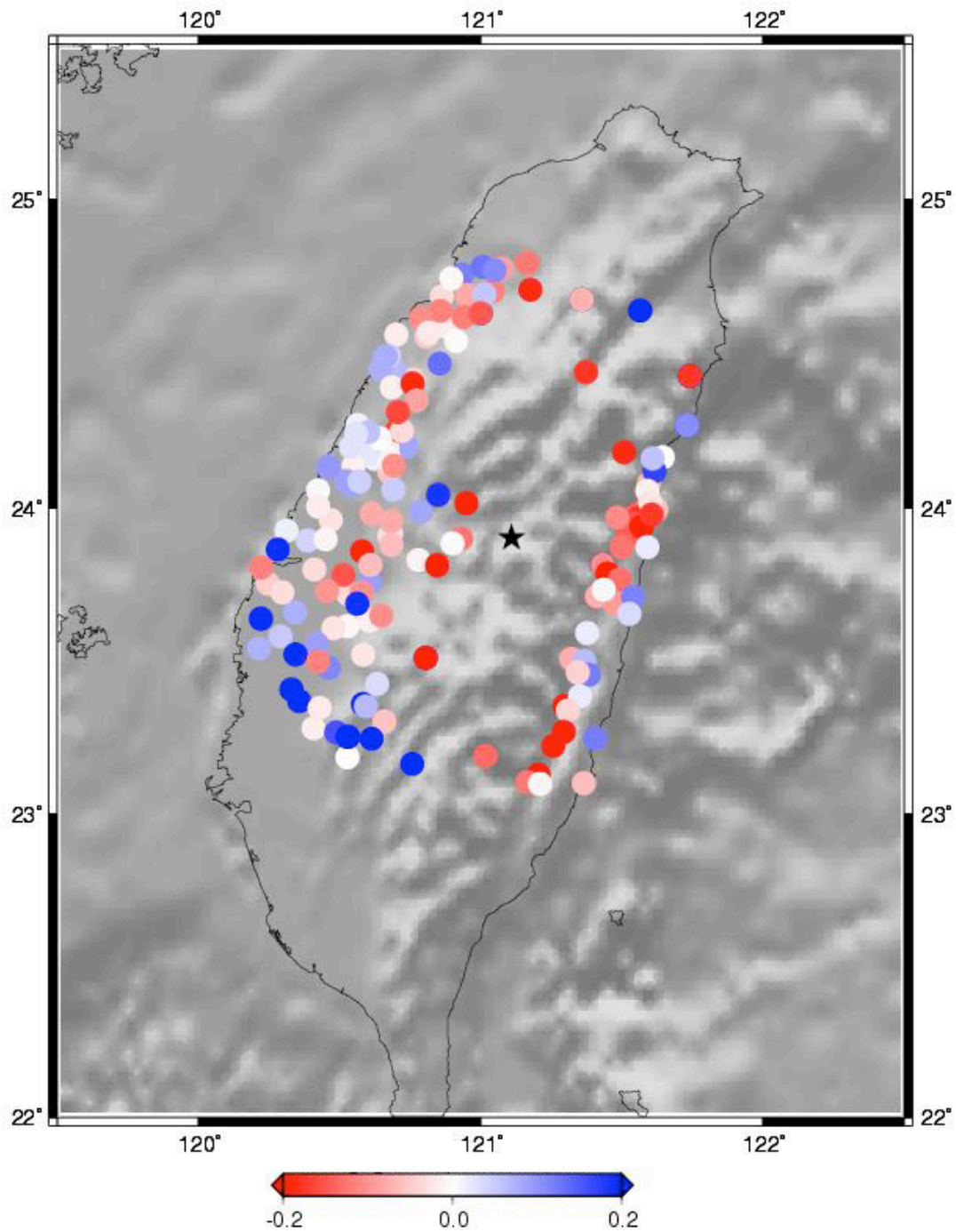


Figure 4. Map of stations within 100km of a M6.4 earthquake that occurred on June 10th 2000. The color scale illustrates $\log_{10}(\tau_p^{\max})$ deviation from the mean τ_p^{\max} for this earthquake.

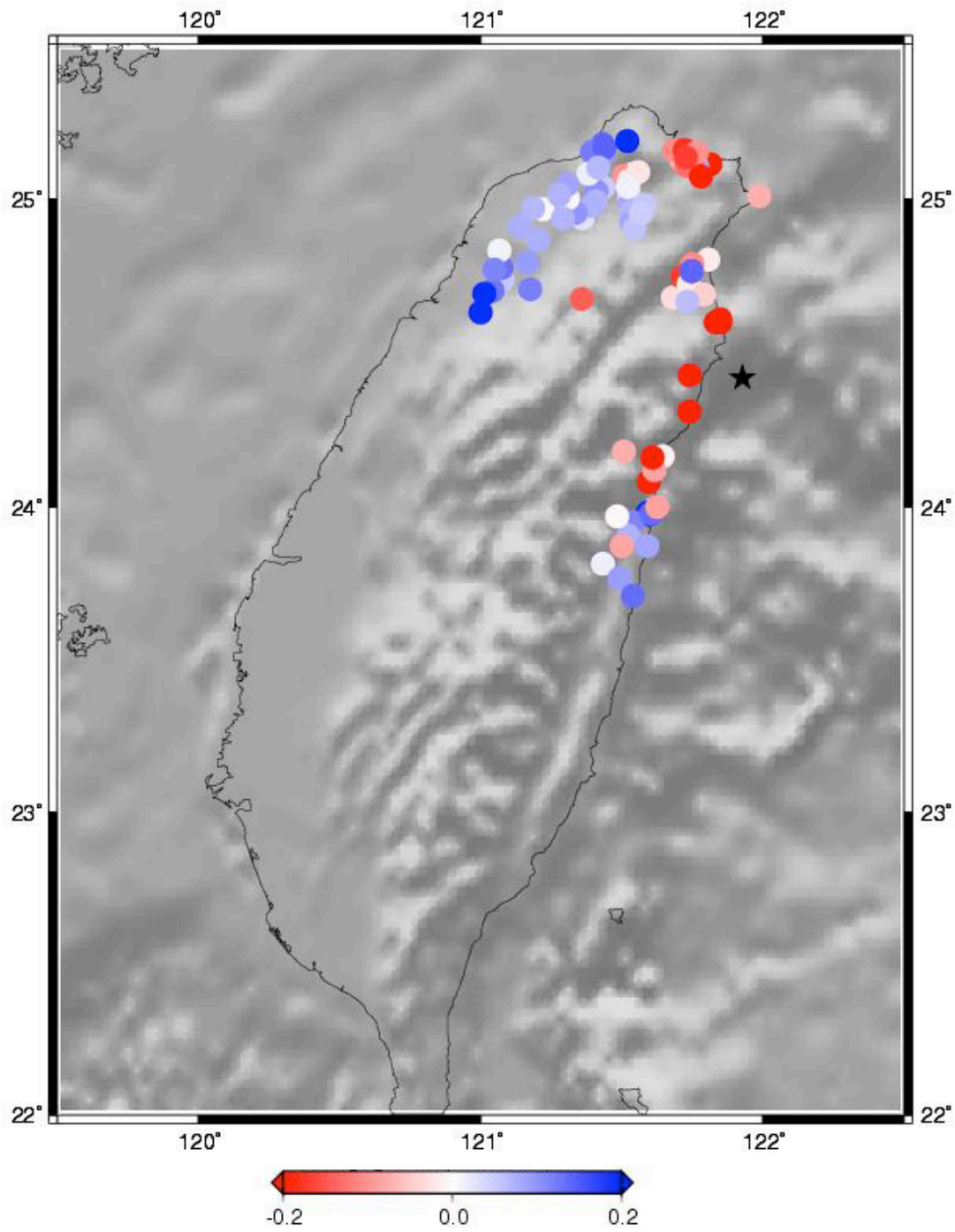


Figure 5. Map of stations within 100km of a M5.9 earthquake that occurred on June 14th 2001. The color scale illustrates $\log_{10}(\tau_p^{\max})$ deviation from the mean τ_p^{\max} for this earthquake.

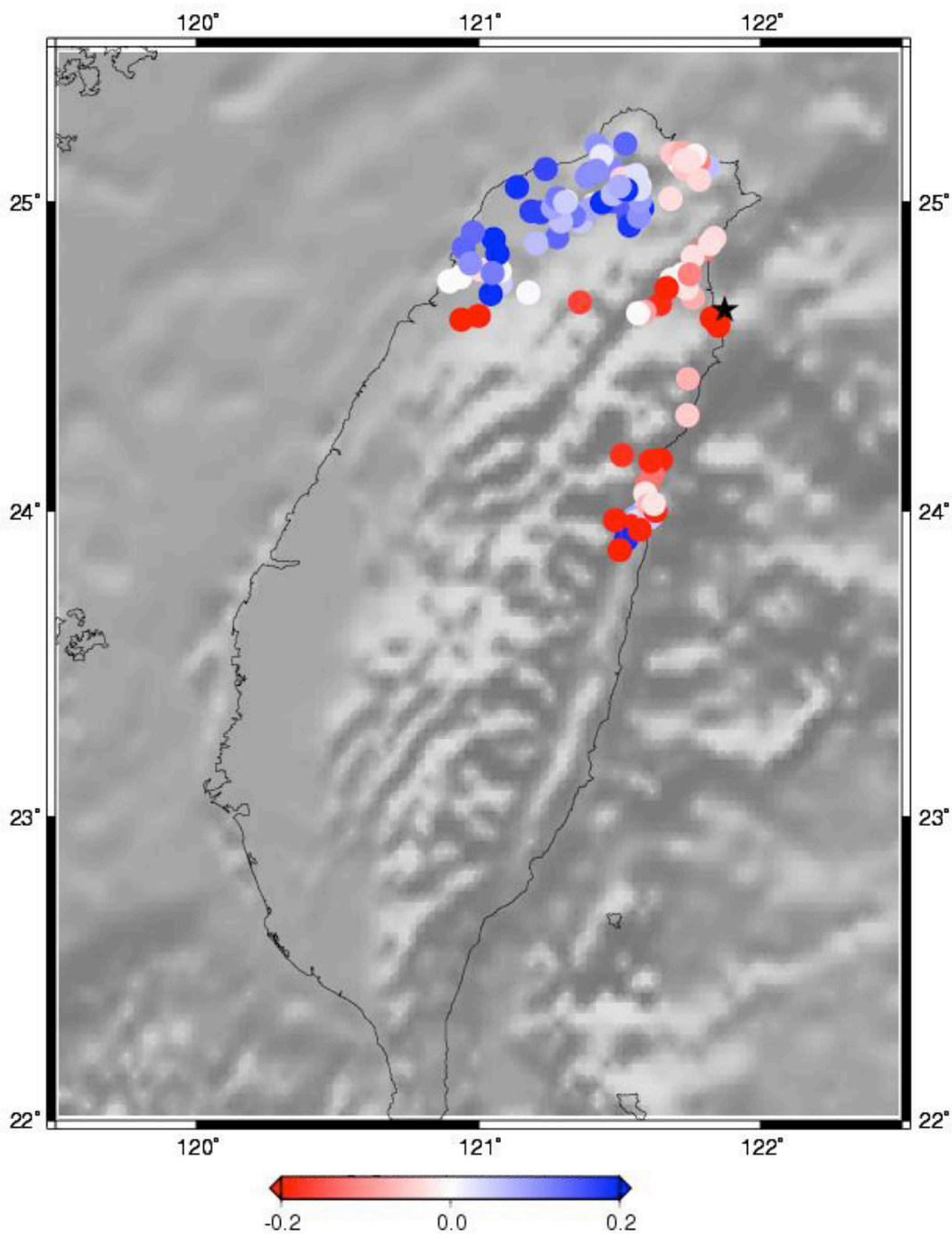


Figure 6. Map of stations within 100km of a M6.1 earthquake that occurred on May 15th 2002. The color scale illustrates $\log_{10}(\tau_p^{\max})$ deviation from the mean τ_p^{\max} for this earthquake.

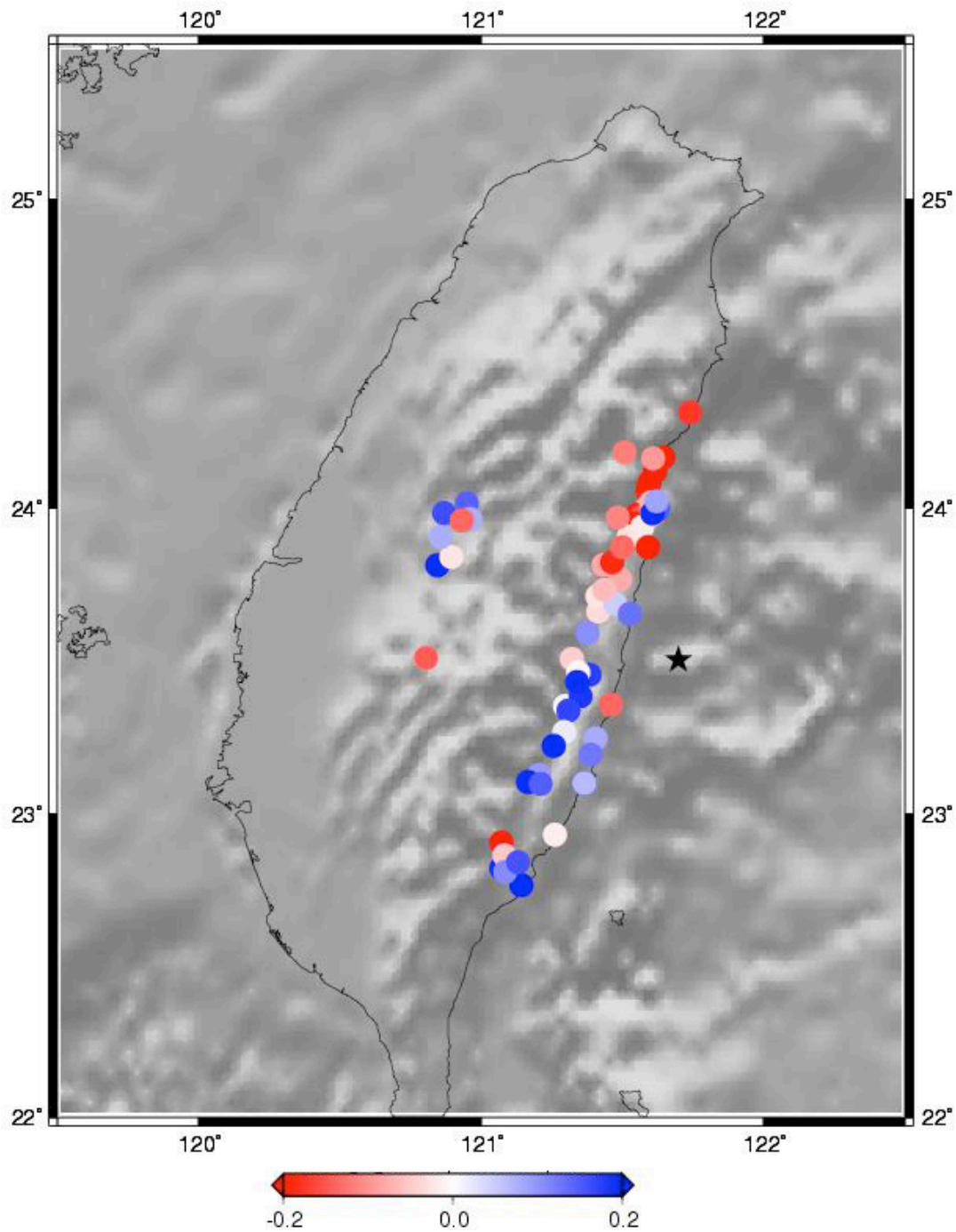


Figure 7. Map of stations within 100km of a M5.9 earthquake that occurred on June 10th 2003. The color scale illustrates $\log_{10}(\tau_p^{\max})$ deviation from the mean τ_p^{\max} for this earthquake.

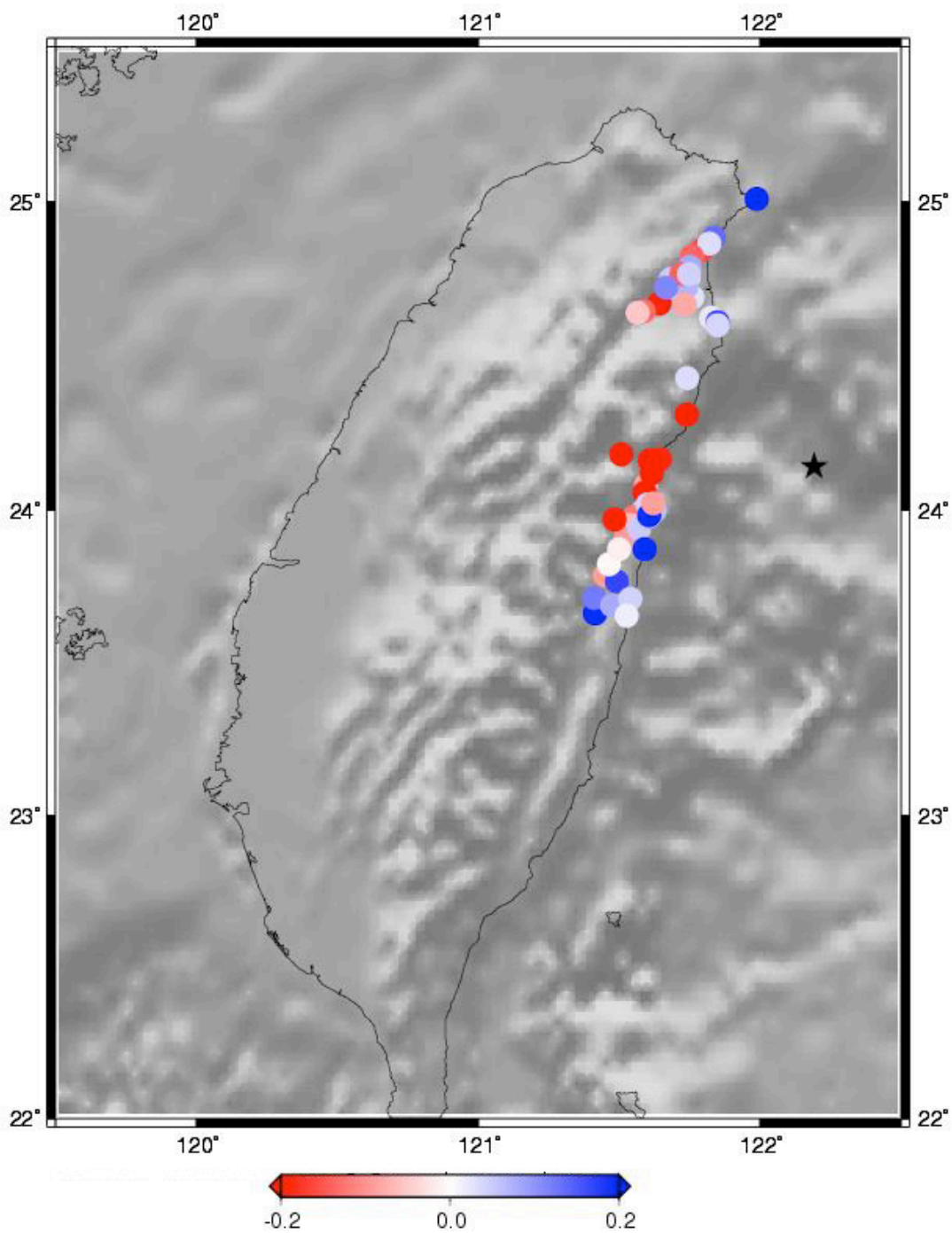


Figure 8. Map of stations within 100km of a M7.1 earthquake that occurred on March 31st 2002. The color scale illustrates $\log_{10}(\tau_p^{\max})$ deviation from the mean τ_p^{\max} for this earthquake.

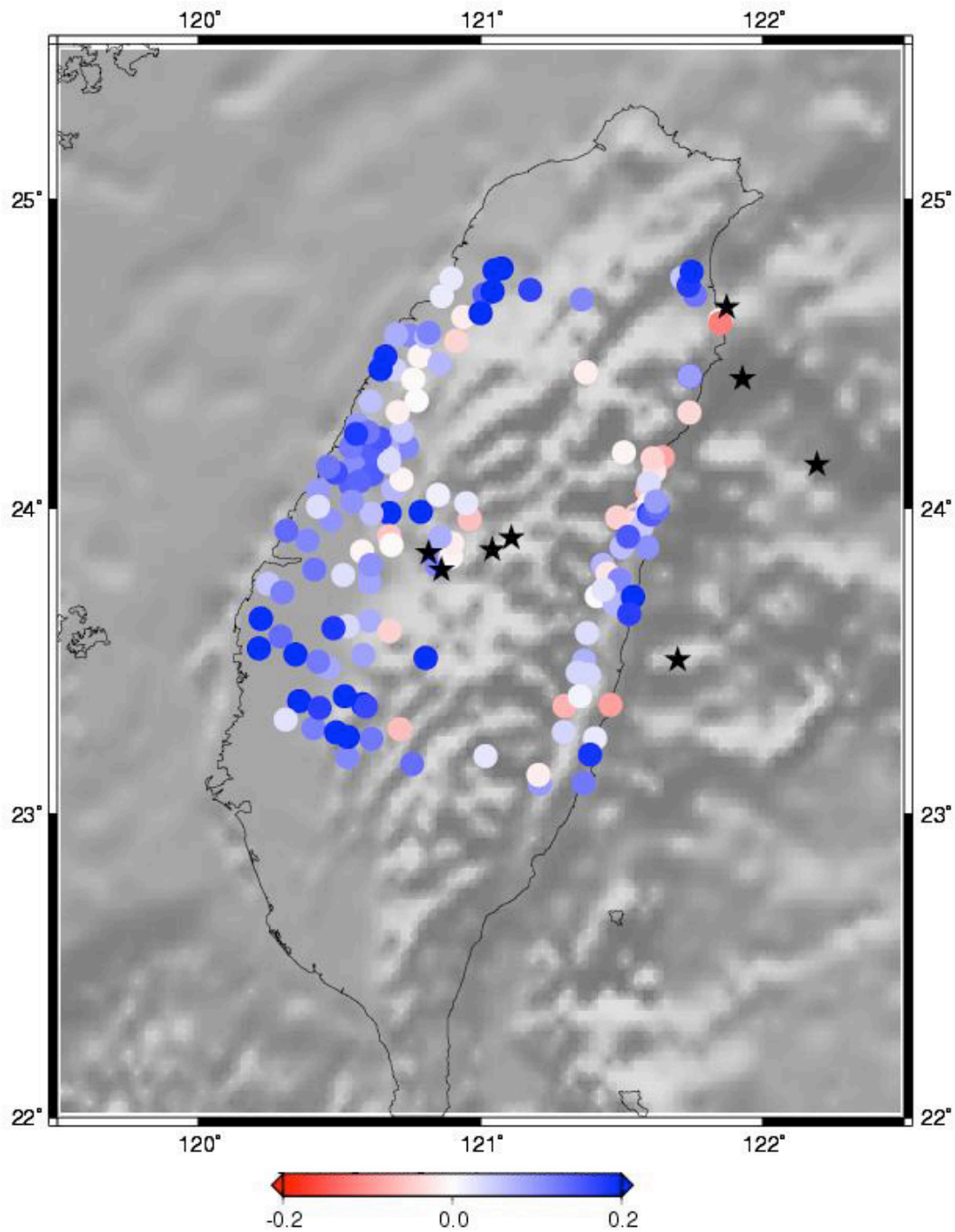


Figure 9. Map of the station correction factors for stations recording 3 or more earthquakes.

The color scale illustrates $\log_{10}(\tau_p^{\max})$ deviation from the mean τ_p^{\max} for this earthquake.

Stars represent the 8 $M_w > 5.9$ earthquakes since 1999.

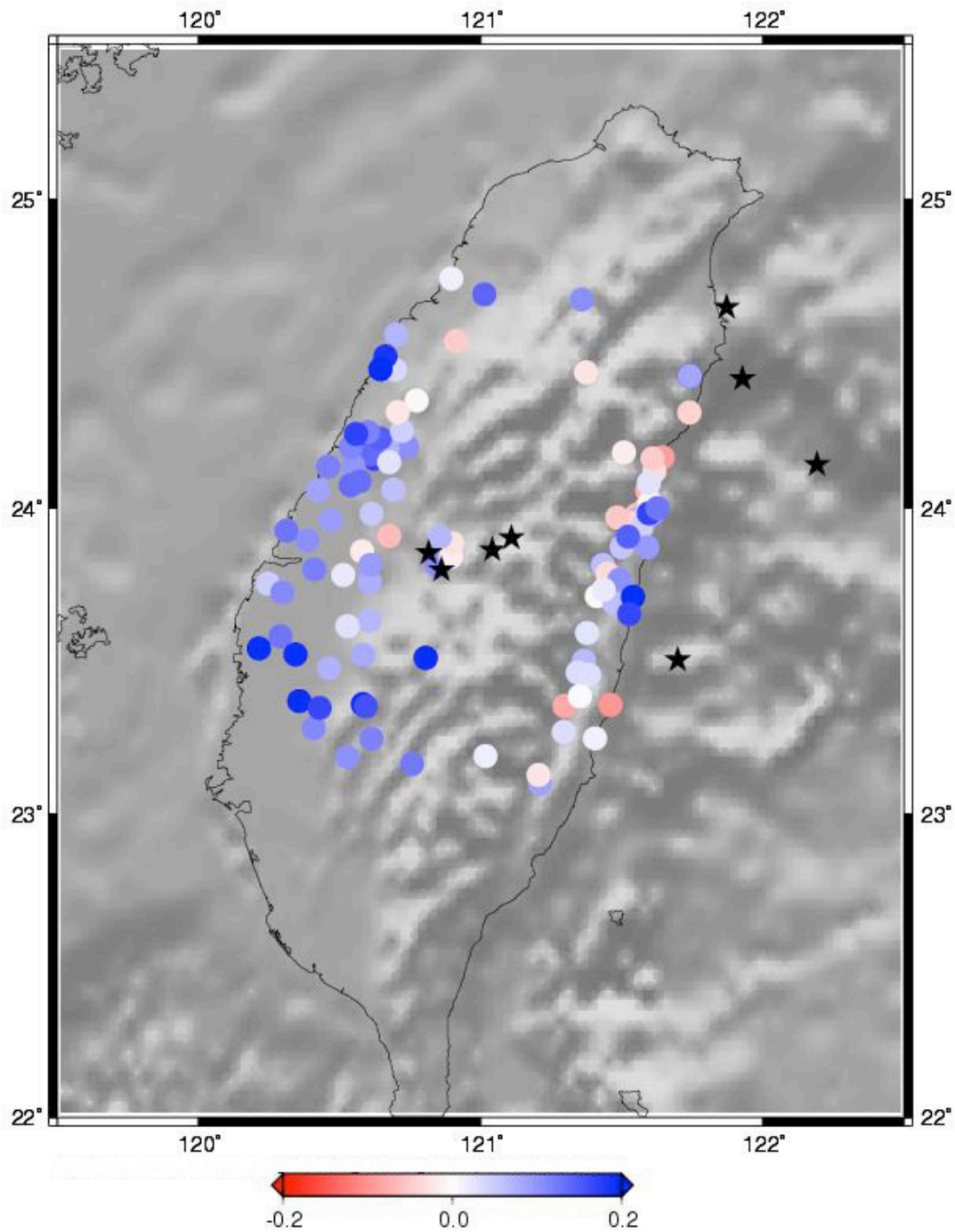


Figure 10. Map of the station correction factors for stations recording 4 or more earthquakes.

The color scale illustrates $\log_{10}(\tau_p^{\max})$ deviation from the mean τ_p^{\max} for this earthquake.

Stars represent the 8 Mw > 5.9 earthquakes since 1999

Table 1: Number of data based on minimum number of events

Minimum number of Events	Number of Data	Number of data from Taiwan	Number of stations From Taiwan
2	1760	859	248
3	1584	683	160
4	1437	536	111
5	1153	252	40
6	1088	187	28

Table 2: Parameters derived from inversion

Minimum number of Events	A $\log_{10}(T_p)/\text{mag}$	B $\log_{10}(T_p)$	Mean absolute station correction $\log_{10}(T_p)$	Mean absolute confidence interval $\log_{10}(T_p)$	Standard deviation $\log_{10}(T_p)$
2	0.1176	-0.6898	0.1461	0.1968	0.1742
3	0.1188	-0.6956	0.1061	0.1731	0.1755
4	0.1229	-0.7144	0.0893	0.1582	0.172
5	0.1315	-0.7549	0.0671	0.1333	0.1669
6	0.1333	-0.7633	0.0688	0.1251	0.1651

CONCLUSIONS AND FUTURE RESEARCH

τ_p^{\max} scales with earthquake magnitude for any earthquake between magnitude 3.0 and magnitude 8.3. The τ_p^{\max} of an earthquake can be measured within the first four seconds of rupture, even if the rupture has not ceased. Previous rupture models that suggested earthquake rupture behaved in a non-deterministic manner cannot explain this new observation, and must be modified, or replaced by a new theory of fault rupture. Earthquake size may be controlled by the location and size of fault patches, or by the amount of slip across these patches at the beginning of rupture. More research into the nature of rupture is required, however before a new hypothesis can be accepted.

Similar to earthquake magnitude, the τ_p^{\max} of an earthquake must be calculated from a waveform recorded by a seismometer. At any point between the fault plane and the seismometer, the τ_p^{\max} value may be altered. Site effects such as regional geology and structure may potentially be corrected for, but alterations to τ_p^{\max} caused by the nature of fault rupture cannot be removed. Taiwan is an ideal location to study possible site effects on τ_p^{\max} due to the large number of stations in the area, and frequent large earthquakes. Unfortunately not enough data from this region has been processed to allow an accurate calculation of station corrections. Evidence suggests site effects do influence the average τ_p^{\max} of an earthquake, but more work is required to understand the size of this influence.

While the previous two chapters represent significant improvements in our understanding of earthquake predominant period, there is still much more we need to learn. Now that τ_p^{\max} is observed as a characteristic of several earthquakes, researchers can study its

properties in a similar way to the study of magnitude, moment, rupture duration, and other earthquake characteristics.

Future research on τ_p^{\max} from several different angles will hopefully lead to a more complete understanding of this phenomenon, and shed light on what causes the τ_p^{\max} signal, and what mechanism controls earthquake size. Some potentially fruitful areas of research include: comparing fault type and rupture mechanism with τ_p^{\max} , studying τ_p^{\max} in more world regions including Iran, Turkey, and Mexico, evaluating τ_p^{\max} teleseismically, examining τ_p^{\max} for small magnitude events, and fully evaluating instrument effects on τ_p^{\max} .

One of the first questions structural geologists ask when they hear about τ_p^{\max} is if there is a relation between τ_p^{\max} and fault type. Does an earthquake on a strike slip fault produce a τ_p^{\max} value different from an event of the same magnitude on a thrust fault? A corollary to that question asks if events with different types of rupture, e.g. dip slip motion on a fault, versus strike slip motion on the same fault, produce different τ_p^{\max} values. Answering both these questions require detailed study of well documented earthquakes, where the fault type and fault motion are both known. Whatever the answer, research in this direction will help develop a stronger understanding of τ_p^{\max} behavior. Broadening the study regions of τ_p^{\max} to a complete global dataset will help when the time comes to set up local early warning systems. Events from Taiwan, Japan, Alaska, and California all follow the same relationship between magnitude and period, but what about events from countries like Turkey, Iran, and Mexico? Recent large earthquakes devastated several regions of Iran, so installing an early

warning system based on τ_p^{\max} could potentially save many lives. However, before such a system can be set up, the relationship between τ_p^{\max} and magnitude must be verified in this region. Therefore pursuing this path of research will not only broaden the community's understanding of τ_p^{\max} , but also potentially benefit the citizens of Iran.

One limitation currently imposed upon τ_p^{\max} is that all stations used to calculate the value must be within 100km from the earthquake epicenter. Over longer distances, attenuation decreases the frequency content of the waveform, resulting in higher τ_p^{\max} values which skew the predominant period trend. However, the maximum useful station distance is unknown, and study of attenuation's effect on τ_p^{\max} may allow stations of greater distance to be included in the calculation of τ_p^{\max} .

In addition to adding more stations at greater distances, a study of τ_p^{\max} at teleseismic distances may find a different τ_p^{\max} relationship. Perhaps there is a threshold frequency lost due to attenuation over a certain distance, so if all the τ_p^{\max} measurements come from beyond that distance they will form a trend that relates to magnitude.

Numerous large magnitude events were added to the predominant period trend in the research presented in chapter 1. However no events with magnitude less than 5.9 were added to the trend. Additionally, all τ_p^{\max} studies to date have only focused on events greater than magnitude 3.0. Part of the reason for this is the threshold noise levels, at which the noise is of similar amplitude to the event. A study of the predominant period for these small magnitude events may allow a lengthening of the magnitude period relationship below

magnitude 3.0, which would strengthen the overall relationship between predominant period and magnitude.

Earthquake prediction is a term to be used with great caution, but the possibility of finding a method for predicting earthquakes entices many geologists. τ_p^{\max} is applicable to early warning, but may also offer a way to predict earthquakes. Unlike previous attempts to predict earthquakes, τ_p^{\max} approaches the problem from a new front, that of frequency content, rather than amplitudes. The beginning of an earthquake is currently defined based on amplitudes. Once the amplitude of ground shaking exceeds the background noise level, an earthquake is said to begin. What if there was a change in frequency content before the change in amplitudes rises above the noise level? Then the earthquake would really begin prior to the amplitude trigger. If the frequency shift is significant, then the earthquake could be detected prior to the traditional trigger, providing fore-warning of ground shaking. This theory could be explored by examining the predominant period over a time window greater than the duration of the waveform. What is the frequency behavior immediately prior to the event? Is the frequency different than a background frequency recorded during quiescence? No one has examined this possibility yet, so the answer remains a mystery.

APPENDIX

Calculating the earthquake predominant period can be a useful step in analyzing the characteristics of an earthquake. τ_p^{\max} of an earthquake contains information about the magnitude of an earthquake, along with clues about rupture properties. However, due to the nature of predominant period calculation, ensuring the correct input parameters is vital to achieving a good measurement. Some of these parameters can vary moderately without a drastic effect, while other parameters must be constrained to 1/100th of a unit.

First, to compare τ_p^{\max} from different events, uniformity is key. Unfortunately with a global data set, and several different magnitude earthquakes, a uniform data set is not easy to compile. Wave, the program that calculated τ_p^{\max} , is constructed to be as flexible as possible with the input data, but there are still limitations. All input data should be recorded at 100 samples/second, especially acceleration data. The need for this sampling rate comes from the real time conversions applied by Wave. In addition, all of the input data should come from stations within 100km of the event epicenter. This constraint is not one of Wave, but rather our current understanding of τ_p^{\max} (see conclusions and future work).

Wave is designed to be a real-time program, able to calculate τ_p^{\max} as an earthquake occurs. While this setup provides the most useful information for early warning, it results in a less than ideal setup for dealing with certain types of data. For acceleration data, rather than simply integrating the entire waveform, the conversion from acceleration to velocity must be done incrementally. This step by step conversion is performed by using an algorithm developed by Kanamori et al. [1999], and requires a few constants to be set prior to the execution of Wave. One such parameter is Q, which affects the filters applied in the

conversion from acceleration to velocity. Extensive testing of Q for 100 sample/second data demonstrated a Q value of exactly 0.994 is best for performing the acceleration to velocity conversion (Please refer to Kanamori et al. [1999] for a more detailed discussion of Q).

There is a trade off with an increase or decrease of Q which affects the similarity between the predominant period calculated from broadband velocity and that calculated from an acceleration derived velocity. This trade off was analyzed by comparing the predominant period calculated from both a strong motion station, and a velocity sensor at the same location, recording the same earthquake. At a Q of 0.994 the two predominant period traces appear most similar, without artificially elevating the predominant period trace. If a sampling rate different than 100 samples/second is to be used, then a new Q would have to be determined by a similar trade off analysis.

In addition to Q, there are two other parameters set in Wave which can yield a different τ_p^{\max} result. The first parameter is the time delay before initiating the search for the maximum point in the predominant period trace. The second parameter is the frequency of the low pass filter applied to all data read into Wave. Here I will discuss the delay time, but for a more detailed discussion of the frequency filter I refer the reader to Lockman and Allen (in review).

The delay time in searching for τ_p^{\max} was implemented to avoid measuring the predominant period of the noise. Predominant period is calculated from the vertical velocity trace using a smoothing constant (refer to the introduction for a more complete description). This smoothing allows for a certain amount of information prior to the current time step to affect the predominant period value at the current time step. This smearing allows the

possibility of the frequency of the noise to affect the frequency measured for the P-wave. After a small amount of time, the smearing is irrelevant, because the only data being combined is that from the P-wave. In the previous studies of τ_p^{\max} , researchers used a delay time of 0.5 seconds, or even 2.0 seconds in some cases [Allen and Kanamori, 2003; Lockman and Allen, In Review; Lockman and Allen, In Review]. However, more research into this delay time suggested that an accurate measurement of the predominant period is available in just 0.05 seconds after the trigger.

Shifting this delay time either earlier or later allows the user to focus on just one region of the predominant period trace. Many larger magnitude events reach their τ_p^{\max} more than 1 second after the trigger, so moving the delay time earlier or later does not substantially affect the calculated τ_p^{\max} . However small magnitude events reach τ_p^{\max} in a much shorter time, sometimes less than 0.1 seconds, so moving this delay time will effect the τ_p^{\max} calculated for small magnitude events. Interestingly, moving the τ_p^{\max} later, to 0.5 seconds, results in a steeper best-fit line, suggesting a more sensitive correlation between magnitude and period at this point (Figures 1 and 2). The reason for this has not yet been uncovered, but remains an area for potential future research.

References Cited

- Allen, R.M., and H. Kanamori, The potential for earthquake early warning in southern California, *Science*, 300 (5620), 786-789, 2003.
- Kanamori, H., P. Maechling, and E. Hauksson, Continuous monitoring of ground-motion parameters, *Bulletin of the Seismological Society of America*, 89, 311-316, 1999.
- Lockman, A., and R.M. Allen, Magnitude Period Scaling Relationships for Japan and the Pacific Northwest: Implications for Earthquake Early Warning, *Bulletin of the Seismological Society of America*, In Review.

Lockman, A., and R.M. Allen, Single station earthquake characterization for early warning,
Bulletin of the Seismological Society of America, in review.

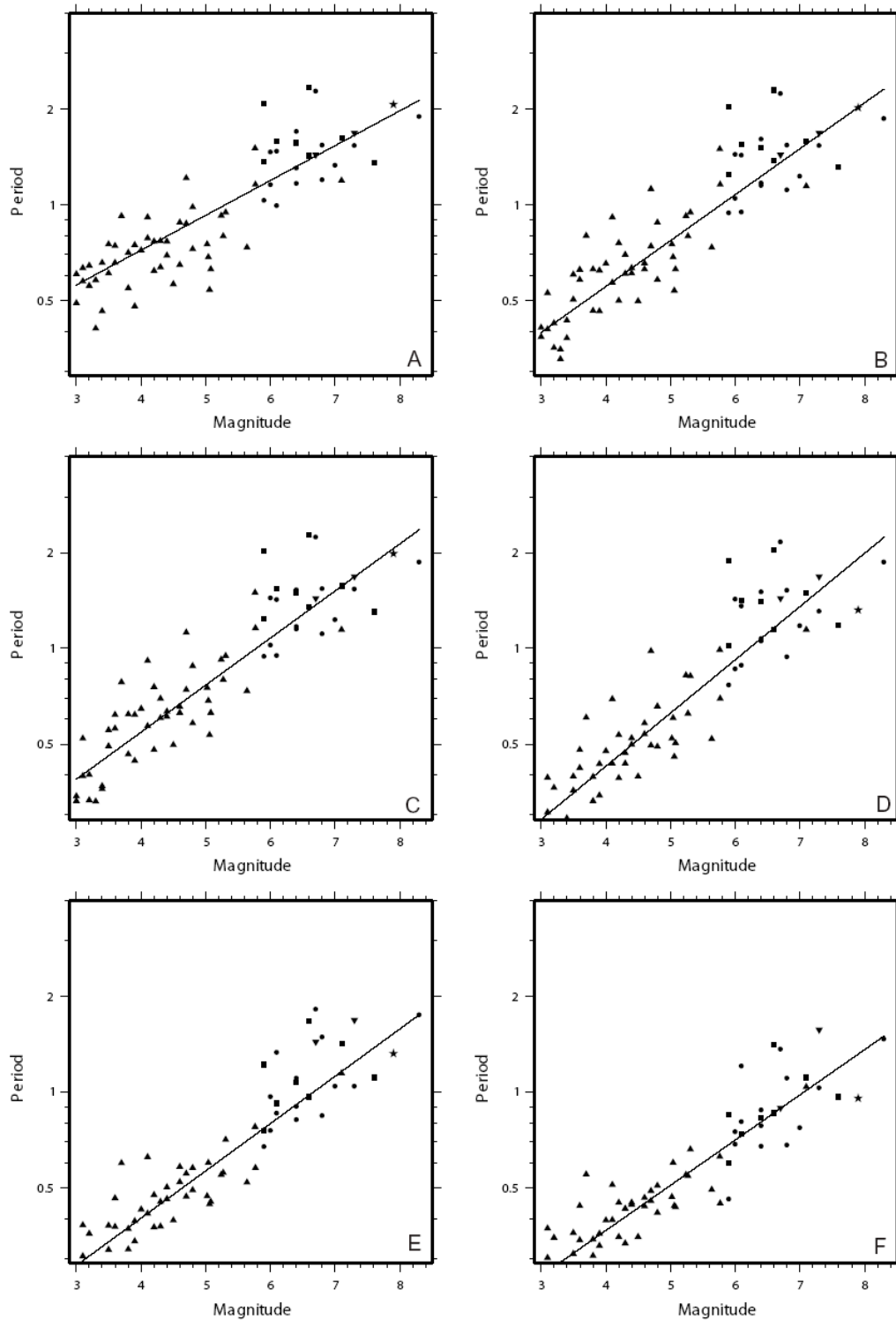


Figure 1. τ_p^{\max} versus magnitude plots for a range of delay times; **a** 0.00 seconds, **b** 0.05 seconds, **c** 0.10 seconds, **d** 0.50 seconds, **e** 1.00 seconds, and **f** 2.00 seconds, after the trigger. Note the change in the slope of the best fit line with increasing delay time.

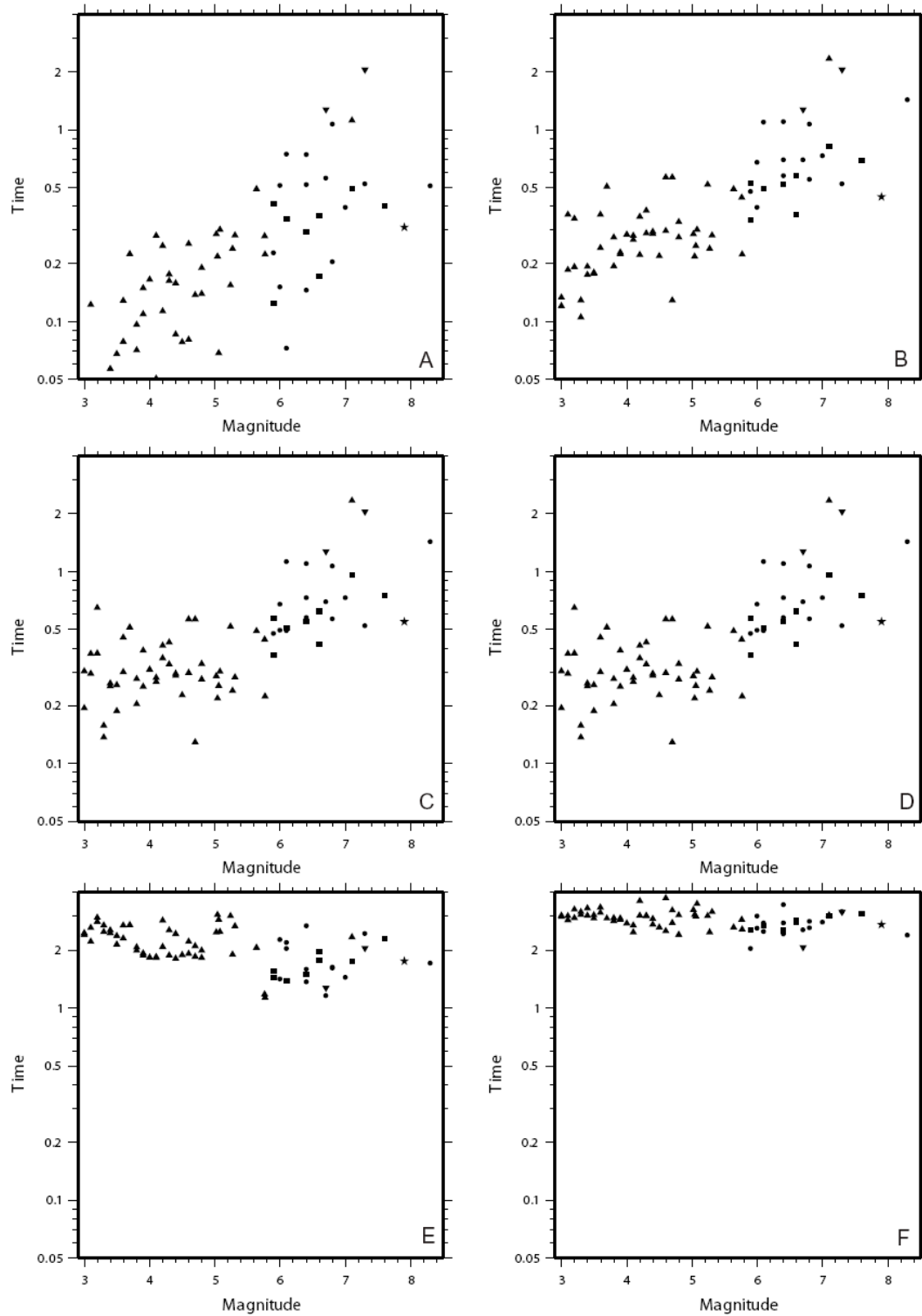


Figure 2. τ_d versus magnitude plots for a range of delay times; **a** 0.00 seconds, **b** 0.05 seconds, **c** 0.10 seconds, **d** 0.50 seconds, **e** 1.00 seconds, and **f** 2.00 seconds, after the trigger. With greater than 1.00 second delay, any meaningful trend is lost.